

EFFECT OF ADHESIVE LAYER ON THE MODE I INTERLAMINAR DELAMINATION OF CFRP BONDED JOINTS

Nassima Nasri¹, Joël Cugnoni¹ and John Botsis¹

¹Faculté des sciences et techniques de l'ingénieur, Ecole Polytechnique Fédérale de Lausanne (EPFL)
Bâtiment ME, Station 9, CH-1015 Lausanne, Switzerland
Email: john.botsis@epfl.ch

Keywords: Energy release rate, Fibre bridging, bonded joints, Asymmetric DCB, delamination

Abstract

In structures made of composite bonded joints, delamination can occur either in the composite or in the adhesive layer. In the first case composite toughness might be affected by the presence of the adhesive, especially if the crack propagates nearby the bond layer. In this work, Asymmetric Double Cantilever Beam (ADCB) bonded joints specimens are tested under mode I to investigate the influence of the adhesive on delamination behavior of CFRP-bonded joints specimens. Experiments showed that the Energy Release Rate (ERR) of the composite is significantly affected by the presence of the bond layer.

1. Introduction

Several structures made of composite material require connections between component members, and for composite structures, the main methods of assembly are bolting and adhesive bonding. The second one has a high potential, since it leads to weight reduction and allows the use of complicated shapes. It also improves the aerodynamic of the aircraft since the surface is smoother than it would be with the use of rivets and bolts. Moreover, the stress distribution is improved around adhesively bonded joints compared to mechanical fasteners since no stress concentrations are introduced.

Despite its many advantages this technique is not extensively applied in this domain because of the lack of knowledge of bonded joints behaviour in terms of durability and fracture toughness, and the difficulty to inspect bondline quality following manufacturing and in-service life. Thus a trustworthy prediction of the strength of the adhesive joints requires reliable material data of adhesives and joining partners. This explains the extensive effort of researchers to develop dependable testing methods in order to obtain the constitutive behaviour of adhesive layers. However, the interaction of an adhesive layer with the propagation of sub-surface delamination cracks within the adherent remains a mechanism which is not well understood.

Experimental works reported in the literature demonstrate that several toughening mechanisms can occur during delamination of FRP composites bonded joints and composite laminates. Fibre bridging for instance occurs when a crack propagates from one fibre/matrix interface to another without breaking the fibre. Experiments show that if the apparent fracture toughness is plotted as a function of crack extension, an increase is observed and this is usually described by a resistance curve (R-curves). In laminated composites, it is shown that this increase is mainly due to the fibre bridging behind the crack tip [1]. In Asymmetric Double Cantilever Beam (ADCB) joints tested in Mode I, the crack propagates in the adherent away from the symmetry plane constituted by the bondline and is therefore accompanied by considerable fibre bridging [2].

Finite Element (FE) analysis is a powerful tool for predicting the fracture behavior of laminated composites and bonded joints. Extensive work on that matter is available [3]. Modeling the effects of the asymmetry and fibre bridging on the fracture behaviour and determination of their influence on Energy Release Rate (ERR) calculations are necessary to accurately describe the fracture behavior of

Nassima Nasri¹, Joël Cugnoni¹ and John Botsis¹

asymmetric adhesively-bonded joints. Among the available methods, the Virtual Crack Closure Technique (VCCT) [4,5] is of interest as it allows determining the mode I and II ERR components G_I , G_{II} , respectively.

This work reports the results of an experimental and numerical study of the influence of an adhesive layer on the mode I interlaminar delamination of ADCB unidirectional composites. Asymmetric specimens made of bulk composite (ADCB-Bulk) are subjected to fracture test and compared to specimens with an adhesive layer layer located several plies underneath the crack starter (ADCB-Joint). Two numerical methods are used to assess the influence of asymmetry on the results and a Cohesive Zone Modeling (CZM) is performed to identify the bridging tractions involved for each configuration.

2. Materials and methods

2.1 Materials

Unidirectional ADCB specimens are produced with 15 plies using the carbon/epoxy prepreg SE70 from Gurit SPTM, with a nominal cured thickness of 0.2 mm. To create a 60 mm asymmetric crack starter in the CFRP bonded joints specimens, a 13 μm -thick PTFE film (A6000 from Aerovac®) is introduced between the 13th and 14th layer. The plate is cured in an autoclave at 80°C with 3 bars pressure for 8 hours, and then cut with a diamond saw to obtain beams with a width of 25 mm. The resulting beams are sandblasted at 4 bars, then cleaned from dust and sand with acetone. The bi-component epoxy adhesive Resoltech 3358T-3350 is used to bond the 3 mm thick CFRP beams, with a special jig designed to ensure a constant bondline thickness of 0.1 mm along the specimen length thus achieving a nominal thickness of 6.1 mm for the final ADCB-Joint specimen. To ensure a complete polymerization of the adhesive the bonded beams are kept under vacuum within the jig during 24 hours and then put in the oven at 70°C during 5 hours. A plate of 6 mm thick ADCB specimens made of bulk composite – without adhesive – is also fabricated by stacking 30 plies of the same prepreg and curing procedure. The following nomenclature is adopted in this work (see Figure 1) DCB2-Joint denotes the bonded specimens with the crack starter between plies 13 and 14 (2 plies away from bondline), while DCB2-Bulk represents the same configuration as DCB2-Joint but without bondline.

All specimens are painted white and marked every millimetre to help monitor the crack tip during crack propagation. Steel loading blocks are glued on the pre-cracked part to obtain ADCB-Joint specimens with the following dimensions: 220x25x6.1 mm and ADCB-Bulk with the following dimensions: 220x25x6 mm.

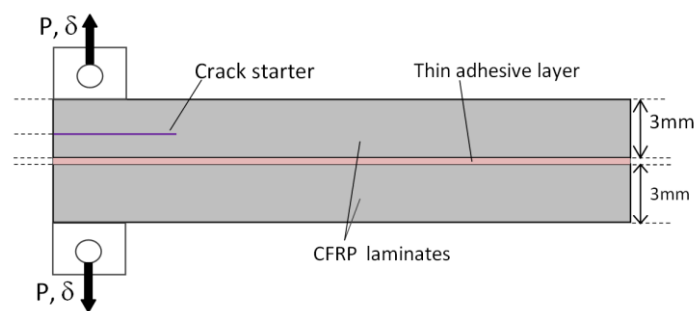


Figure 1: Asymmetric DCB bonded joint specimen

2.2 Monotonic test and data reduction method

Tests are conducted in an Instron 5848 machine with a 2kN load cell. The specimens are subjected to monotonic (1 mm/min) mode I loading in displacement control, following the tests procedure of the

ASTM standard D5528-03 [7]. A high resolution CCD camera is used to monitor the crack propagation during delamination by taking pictures at 1 Hz of the marked side of the specimens. The total ERR, G_{total} , is calculated using the following expression:

$$G_{total} = \frac{P^2}{2B} \left(\frac{\partial C}{\partial a} \right) \quad (1)$$

where P is the load, C is the compliance, a is the crack length and B the specimen width. The compliance is fitted by the following power law, which is a modified version of the compliance calibration method [7]:

$$C = B(a + D)^m \quad (2)$$

where B , D and m are fitting parameters. Independent measurements of the ERR are carried out using the J-integral $J = P\theta/B$ where θ is the relative angle between the arms of the DCB specimen measured by digital image correlation. Comparison of these measurements and the ones given by (1) show very small differences thus, geometrical nonlinearities are considered negligible.

2.3 Numerical analysis

Three different modeling approaches are used in a FE model using the software Abaqus®. All models are 2D plain strain models, with the 20 μm thick initial crack contained in the upper beam.

(a) VCCT method

Since the crack starter is not placed at the midplane of the asymmetric DCB specimens, the asymmetry may cause a non negligible component of mode II even during mode I loading. A numerical study using the VCCT method has been carried out to quantify the amount of mode II as a function of the crack starter position.

(b) J-integral calculation

2D models of DCB2-Bulk and DCB2-Joint have been realised to compare the J-integral values of the bulk and joints configurations, without bridging but with the elasto-plastic behavior of the adhesive layer taken into account. The properties of the adhesive are obtained from dogbone tests performed according to the ASTM D368 [8]. The crack front is modelled with a radial mesh using singular elements. The mesh is refined close to the crack tip and calculation of at least 10 contours integrals are carried out for each configuration. The simulations are performed with displacement control at the loading pins.

(c) Fibre bridging model with joint plasticity

The first step is the identification of bridging tractions. The configurations DCB2-Bulk and DCB2-Joint are simulated with 2D-plane strain models. For DCB2-Joint simulation, the composite and the adhesive layer are introduced as separate parts tied together. A seam is introduced to simulate the crack and quadrilateral elements with reduced integration (CPE8R) are used. Elements are collapsed at the crack tip and their mid-nodes are shifted to $1/4$ of the edge to create a $1/\sqrt{r}$ singularity (r being the distance from the crack tip). A parametric surface traction $\sigma_b(z)$ is implemented to represent the bridging zone as follows:

$$\sigma_b(z) = e^{-\gamma z} \left(\sigma_{\max} - \frac{\sigma_{\max}}{z_{\max}} z \right), \quad 0 \leq z \leq z_{\max} \quad (3)$$

where γ is an identified parameter taking into account the non linearity of the tractions, σ_{\max} is constant ($=1.39\text{MPa}$ at $z = 0[1]$) representing the maximum tractions at the crack tip, and z_{\max} is the maximum bridging length, extracted from the experimental results of time vs. crack length when crack length becomes a linear function of time. The Crack Opening Displacements (CODs), $\delta(z)$ extracted from the numerical model, are then combined with the bridging tractions $\sigma_b(z)$ to obtain $\hat{\sigma}_b(\delta)$.

The contribution of bridging $G_{I,b}$ to the total ERR, G_{total} is calculated with the following equation [9]:

$$G_{total} = G_{I,i} + G_{I,b} = G_{I,i} + \int_0^{\delta_{\max}} \hat{\sigma}_b(\delta) d\delta \quad (4)$$

where $G_{I,i}$ is the ERR at initiation and δ_{\max} is the COD at the z_{\max} , i.e. the end of the bridging zone. In this case, as all other parameters are known only γ is identified so that the numerical integration $\int_0^{\delta_{\max}} \hat{\sigma}_b(\delta) d\delta$ corresponds to the contribution of bridging $G_{I,b}$. The identified bridging law of each configuration (one for DCB2-Bulk and one for DCB2-Joint) is appended to a linear degradation cohesive traction-separation relationship representing matrix cracking. A 2D-cohesive elements model is finally used to predict the load-displacement curve, through a tabular multi-linear damage evolution law in Abaqus for crack propagation simulation.

3. Results and discussion

3.1 Experimental results

Typical load-displacement curves from DCB2-Bulk and DCB2-Joint are shown in Figure 2. For clarity of presentation, the initial jump occurring at the precrack stage to propagate the crack further the resin rich region has been omitted. Those curves suggest a different mechanism at initiation since the onset of non linearity, correlated to the onset of crack propagation, occurs at a higher load for the joint. Moreover, the decrease of the load is sharper for joint than for bulk specimens, indicating a lower fibre bridging leading to a lower G_{total} at steady state for joints compared to bulk specimens.

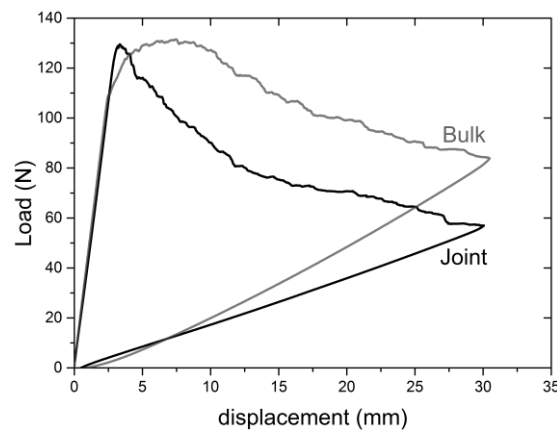


Figure 2: Comparison of load-displacement curves from DCB2-Bulk (gray) and DCB2-Joint (black)

The calculated resistance curves for each configuration are shown in Figure 3.

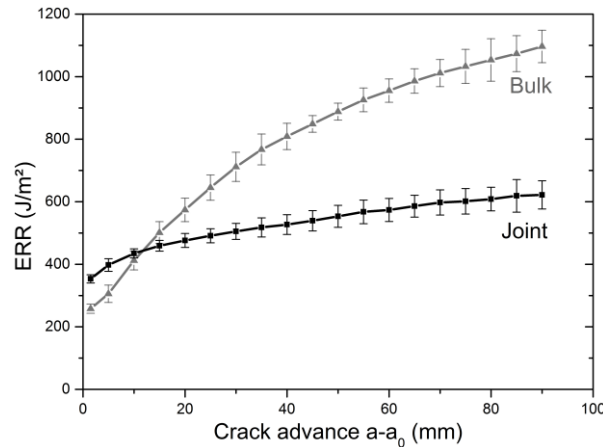


Figure 3: Average R-curves for DCB2-Bulk and DCB2-Joint specimens

As indicated from the load displacement curves comparison, the fracture toughness at initiation is highly influenced by the presence of the adhesive layer: $G_{I,i} = 270 \text{ J/m}^2$ for DCB2-Bulk while $G_{I,i} = 350 \text{ J/m}^2$ for joints. This difference of 80 J/m^2 has to be correlated with a different failure mechanism at the interface matrix/fibre level. Indeed, observations with both an optical microscope (magnification x20) and an SEM (magnification up to x2000) clearly show that the failure mechanism is different: in the case of bulk specimens the crack propagation leaves most of the fibres clean of matrix, indicating a failure at the interface matrix/fibre, whereas the fibres seem to be covered with resin for joints specimens, indicating a matrix failure probably occurring at the resin rich region. Thus the differences of $G_{I,i}$ between bulk and joints are attributed to material heterogeneities at the crack starter.

The initiation is followed by a typical R-curve behavior for the bulk specimens, whereas the ERR value for joints specimens increases much less. The large difference of ERR at steady state between bulk and joints which is over 400 J/m^2 , can be explained by the different amount of fibre bridging involved in the process. Indeed, micro sections (see Figure 4) of bulk and joints specimens show that when there is the adhesive layer, only isolated fibres are involved in the fibre bridging, while many substantial bundles connect the two arms in the case of bulk composite. Bundles of fibres require more energy to break than isolated fibres, leading to a very different R-curve behavior and ERR value at steady state.

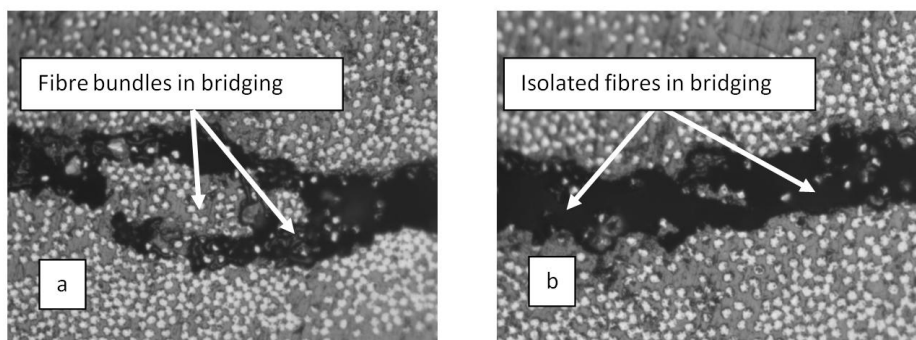


Figure 4: Micro sections of a) ADCB-Bulk specimen and b) ADCB-Joint specimen after delamination 5mm from the crack tip

Experimental results show that the adhesive is mainly responsible for the observed change in ERR during propagation and not the asymmetry. The ERR at steady state for ADCB-Joint is 650 J/m² while the ERR of an ADCB-Bulk is about 1000 J/m². The ERR of a symmetric DCB specimen made of bulk composite is also 900 J/m² [1]. This proves that the asymmetry is not responsible for the important change of toughness properties of the ADCB-Joint thus, the mechanisms involved in the fibre bridging are heavily influenced by the presence of the joint.

3.2 Numerical Modeling results

3.2.1- VCCT results

The results in Figure 5 show that the mode II component remains negligible (<4%) for configuration DCB1-Joint (crack 1 ply away from adhesive) and DCB2-Joint but reaches 10% for joints when the crack starter is 3 plies from the midplane. The mode II component is higher for joints than for bulk composite specimens. Note that only the configuration DCB2 is experimentally realized. However, those simulations do not take into account the fibre bridging mechanism, which dissipates a significantly larger amount of energy and can induce large changes in the mode mixity at crack tip. Therefore the 10% of mode II contribution at initiation may become negligible when bridging is developed. Digital image correlation measurement of the normal and shear COD at crack tip confirmed this hypothesis. Consequently, the mode II component can be neglected for the configurations DCB1, DCB2 and DCB3, confirming the results found in the literature [2,10].

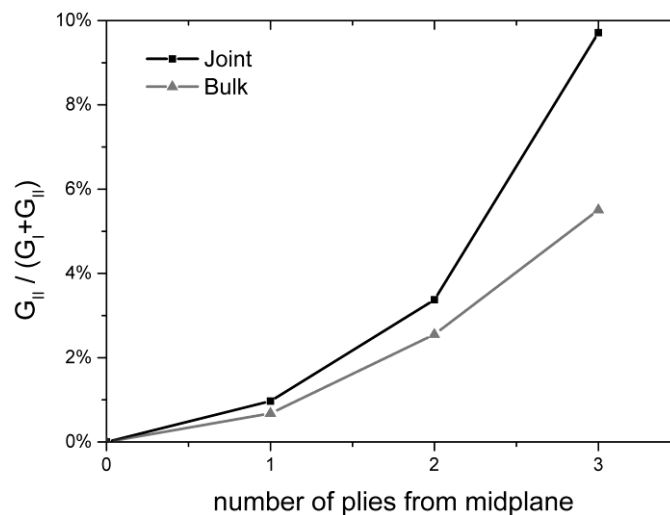


Figure 5: Mode II ratio as a function of crack starter position for DCB specimens with and without bondline

3.2.2. J-integral : elastic model without bridging

The contour integrals extracted from models of DCB2-Bulk and DCB2-Joint did not show a significant difference. Also no difference in terms of stress at the crack tip was observed in the models between joints and bulk specimens. Nevertheless these models showed that the stress field applied to the adhesive layer is high enough to produce plastic strain in the bondline. This plasticity occurring in the adhesive layer might affect the energy available for the crack propagation, interfering with the bridging fibre phenomenon.

3.2.3 Cohesive zone model

Parameters γ and z_{max} identified in the bridging law for the DCB2-Bulk are respectively 0.09 and 60 mm, hence in good agreement with the scale functions introduced by Farmand-Ashtiani et al [1]. That means that the DCB2-Bulk configuration is similar to symmetric DCB-Bulk specimen, confirming that the asymmetry does not play an significant role.

The identified parameters γ and z_{max} for the DCB2-Joint, 0.24 and 60 mm respectively, are used to predict the load displacement curve for the same crack length and displacement as in experimental conditions (see Figure 6). Based on the cohesive simulation with plastic bondline, it is found that the amount of energy dissipated by plastic deformation of the adhesive layer is very small (see Figure 7) compared to the total work of external forces involved in the process (less that 1.5%). Consequently this model shows that the plasticity of the adhesive layer cannot energetically explain the change of behavior between joints and bulk composites.

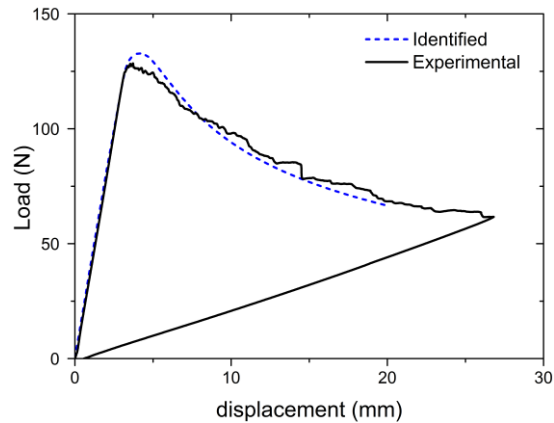


Figure 6: Experimental and numerical load displacement response of DCB2-Joint

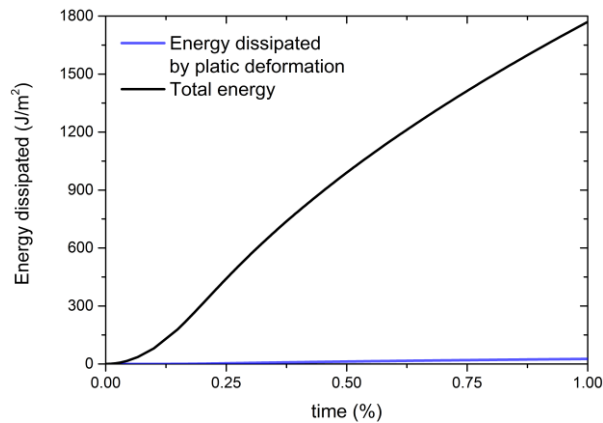


Figure 7: Energy distribution from the CZM FE model of DCB2-Joint

4. Conclusions

Fracture behavior of asymmetric DCB unidirectional CFRP laminate was studied with and without the presence of an adhesive layer close to the crack plane. Results show that the bond layer significantly affects the fracture toughness of the composite. The numerical methods VCCT and J-integral were used to assess that the mode II component is negligible, and thus the mode mixity is not responsible for this change of behavior. The latter model also showed that the adhesive layer is submitted to a stress sufficient to induce plasticity thus the hardening curve of the adhesive was extracted from dogbone tests and added to the material properties in the model, though the non linear behavior of the adhesive does not significantly affect the stress field at the tip. The bridging laws for both bulk and joint configurations have been identified and exhibit significantly different bridging parameters. Cohesive elements simulations were performed and found to fit the load displacement curves very

well for both cases. An energetic analysis extracted from the cohesive elements models showed that the plasticity occurring in the bond layer is not responsible for the change of toughness properties of the composite. Transversal sections of the specimens were observed with an optical microscope and showed that the fibre bridging is composed of bundles of fibres in the case of bulk composite specimens, while isolated fibres connect the two arms of bonded joints. As fibre bundles require more energy to break than isolated fibres, it was ascertained that the difference of bridging is responsible for the change of behavior.

References

- [1] E. Farmand-Ashtiani, J. Cugnoni, and J. Botsis, 'Specimen thickness dependence of large scale fibre bridging in mode I interlaminar fracture of carbon epoxy composite', *International journal of solids and structures* 2015, vol. 55, p. 58-65.
- [2] Moslem Shahverdi, Anastasios P. Vassilopoulos, Thomas Keller. A phenomenological analysis of Mode I fracture of adhesively-bonded pultruded GFRP joints. *Engineering Fracture Mechanics*, 2011, pp. 2161–2173.
- [3] Tay, TE. Characterization and analysis of delamination fracture in composites: An overview of developments from 1990 to 2001. 2003, *Appl Mech Rev*, Vol. 56
- [4] Xie D, Biggers SB. 11. Progressive crack growth analysis using interface element based on the virtual crack closure technique, 2006, *Finite Elem Anal Des*, Vol. 42, pp. 977–984.
- [5] R., Krueger. The virtual crack closure technique: history, approach and applications. *Appl Mech Rev*, 2, 2004 Vol. 57, pp. 109-143.
- [6] Moslem Shahverdi, Anastasios P. Vassilopoulos, Thomas Keller. Modeling effects of asymmetry and fiber bridging on Mode I fracture behavior of bonded pultruded composite joints. 2013, *Engineering Fracture Mechanics*, Vol. 99, pp. 335–348.
- [7] ASTM D5528 – 13, 2007. *Standard Test Method for Mode I Interlaminar Fracture Toughness of Unidirectional Fiber-Reinforced Polymer Matrix Composites*
- [8] ASTM D638 – 10, 2010. *Standard Test Method for Tensile Properties of Plastics*.
- [9] Rice J., A path independent integral and the approximate analysis of strain concentration by notches and cracks, 1968, *J. Appl. Mech.* Vol 35, p.379-386
- [10] V. Mollón, J. Bonhomme, J. Viña, A. Argüelles. Theoretical and experimental analysis of carbon epoxy asymmetric dcb specimens to characterize mixed mode fracture toughness. 2010, *Polymer Testing*, Vol. 29, pp. 766-770